Proceedings of the 25th International Conference on
Port and Ocean Engineering under Arctic Conditions
June 9-13, 2019, Delft, The Netherlands

Local Ice Load Prediction Formulas Based on Arctic Field Measurements of the IBRV ARAON

Sungrok Cho[1], Kyungsik Choi[1]
[1] Department of Ocean Engineering, Korea Maritime and Ocean University, Busan, Korea

ABSTRACT

This paper describes a procedure to derive the pressure-area type ice load prediction formulas by applying probabilistic approach based on the Arctic field test data from the icebreaking research vessel, ARAON during 2016 Arctic voyage. Strain gauge signal from ARAON's hull plating was converted to calculate the local ice pressure upon the hull plating using the influence coefficient matrix and finite element analysis for the hull structures of ARAON. Besides the strain gauge records, data for the ship speed and ice thickness during the ship-ice collision processes were also measured. Adopting a concept of collision 'event' and probability of exceedance function, the peak values of ice pressure on the designated area of local hull plating are analyzed to develop a modified pressure-area relationship. Derived local ice load prediction formulas show the practical variation of pressure-area relationship according to the different speeds and different sea ice thicknesses.

KEY WORDS Local Ice Load Prediction; Arctic Field Test Data; Probabilistic Approach; Pressure-Area Relationship; Icebreaker ARAON

1. Introduction

One of the important factors in the design of an icebreaking vessel is to determine a reasonable design ice load in practice however it is difficult to quantify the correct ice loads.

Prediction formulas for local ice loads are usually described as functions of contact area, so called the pressure–area relationship. Many researchers derived pressure-area relations for offshore structures and ships in various conditions (Masterson and Frederking, 1993). Previous local ice load predictions involving contact areas can be used for design of structural members, however it may be practical to include other factors such as contact speeds, ice thickness etc. for prediction of local ice loads.

In this study, with an appropriate probabilistic approach (Frederking, 2004; Jordaan et al., 1993; Taylor et al., 2010), traditional P-A type ice load prediction formula is modified to consider ship speed and ice thickness, based on the Arctic field test data from the IBRV

ARAON's 2016 Arctic voyage.

2. Arctic field data of the IBRV ARAON

The Korean icebreaking research vessel, ARAON has been used for gathering ice load data in the Arctic Sea every summer since 2010. In August 2016, the ARAON performed several field tests in the Chukchi and Beaufort Seas. During field tests, strain data was recorded from strain gage sensors installed on the hull plating and the transverse frames of ARAON's bow area. Information such as ship motion including ship speed, ice properties and ice thickness were also collected from various sensors and the integrated monitoring system.

In the port side of the ARAON's hull plating inside bow thrust room, a total of 8 single strain gages, 20 rosette gage sensors were installed and in the starboard side, 12 rosette gage sensors were installed as shown in Figure 1.

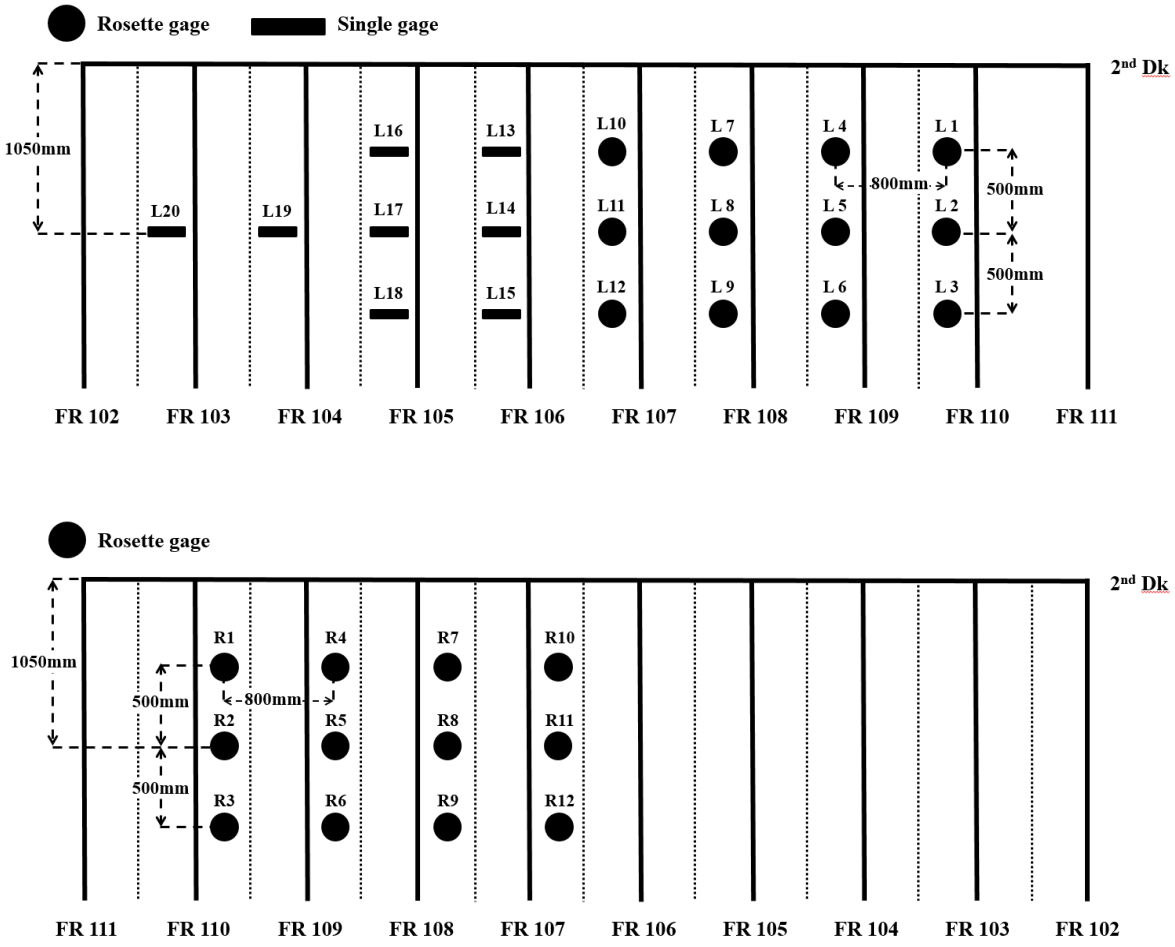

Figure 1. Position of the installed strain gauges on the hull plates of the ARAON

In case of single gages, a uniaxial stress-strain relationship is used for calculating stresses.

$$\sigma_x = E \times \epsilon_x \tag{1}$$

where ϵ_x is the measured strain in longitudinal direction and E is the modulus of elasticity.

In case of 3-axis rosette gages, Eq.(2) and Eq.(3) calculate principal stresses, σ_1 and σ_2 from the measured strains and the von Mises equivalent stresses can be calculated using Eq.(4).

$$\sigma_1 = \frac{E}{2(1-\upsilon)}(\epsilon_A + \epsilon_B) + \frac{E\sqrt{2}}{2(1+\upsilon)}\sqrt{(\epsilon_A - \epsilon_C)^2 + (\epsilon_B - \epsilon_C)^2} \tag{2}$$

$$\sigma_2 = \frac{E}{2(1-\upsilon)}(\epsilon_A + \epsilon_B) - \frac{E\sqrt{2}}{2(1+\upsilon)}\sqrt{(\epsilon_A - \epsilon_C)^2 + (\epsilon_B - \epsilon_C)^2} \tag{3}$$

$$\sigma_{eq} = \sqrt{\sigma_1^2 + \sigma_2^2 - \sigma_1\sigma_2} \tag{4}$$

where υ is the Poisson's ratio.

Calculated stresses are converted to produce the ice pressure upon the hull plating using the influence coefficient matrix and finite element analysis for the hull structure (Lee et al., 2013). The size of shell plating covered by one strain gage is 800×500mm. Therefore, for port side $8m^2$ corresponding to 20 strain gages is defined as the total local area. For starboard side, $4.8m^2$ corresponding to 12 strain gages is defined as the total local area.

Ship speed was measured using a GPS installed outside the hull structure near centerline of the ship. Information for sea ice thicknesses is obtained using image processing software and video images of the broken ice pieces (Park et al., 2014; Figure 2). Video camera, installed on starboard side near midship, records the image of up-turned broken ice pieces to estimate the ice thickness. Adjustment to synchronize the GPS, video camera images and strain gage signals is necessary due to the different position of the installed equipment.

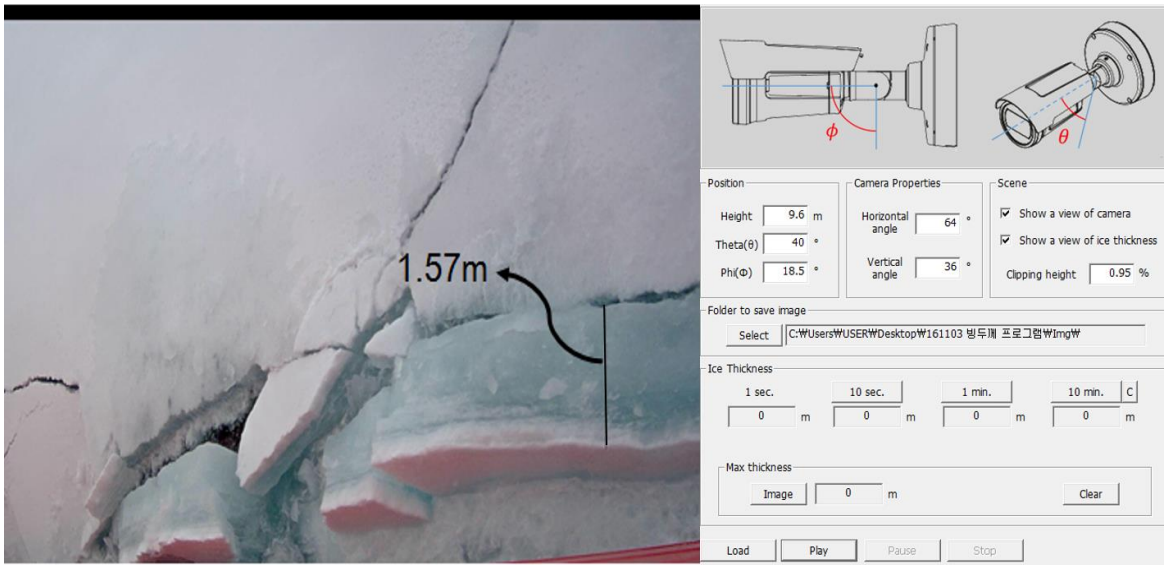

Figure 2. Image processing software to estimate sea ice thicknesses (Park et al., 2014)

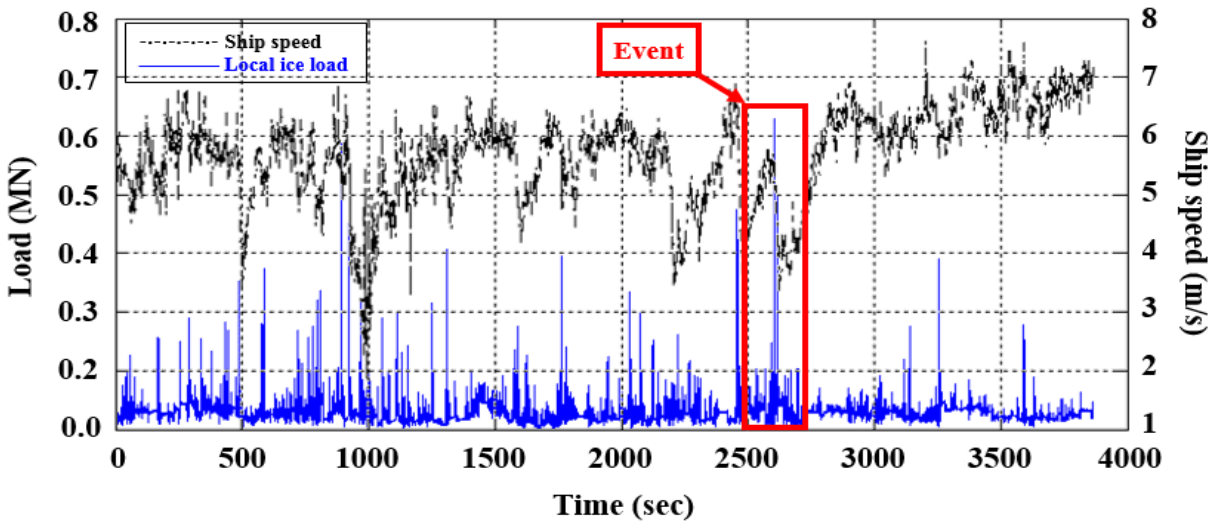

Figure 3. Time history of calculated local ice loads and measured ship speed (Jeon et al., 2017)

In Figure 3 the calculated local ice loads and measured ship speed are shown over time. Here the concept of 'event' is adopted to sort out peak ice pressures. This concept is well described in previous study (Min et al., 2016). When a ship collides with large ice feature, the speed of ship sharply decreases as ship penetrates into the ice. Contrary to decreasing ship speed, the ice load increases to a certain peak value and then ice fails. As shown in Figure 3, the time history of local ice load estimated by summing pressures at the strain gage locations can be divided into a series of events. It is possible to select one peak ice load and one incoming ship speed during each event. In this study, an event is defined when ice load above the threshold occurs at these sections. The threshold was set to 0.4MN for 2016 ice load data. The total number of events is 1,712.

3. Probabilistic approach and P-A relationship

Even though the global average pressure decreases with area, there can be areas within the total area which are subjected to high local pressures. The design of local areas within a structure corresponds to different definition of area.

The probabilistic approach to derive an area-dependent local ice load prediction formula was previously studied by several researchers (for example Frederking, 2004; Jordaan et al., 1993; Taylor et al., 2010). In this paper a similar approaches are adopted for producing a pressure-area relationship especially for the IBRV ARAON.

Peak ice pressure data in each collision event are arranged in descending order for each area and are plotted against $-ln\left(\frac{i}{n+1}\right)$ where i is the rank of the pressure and n is the total number of events producing pressures greater than a threshold value.

Tail of the distribution can be represented by an exponential distribution of the form

$$P_e = exp(-\frac{x - x_0}{\alpha}) \quad (5)$$

where x is a random quantity denoting ice pressure as shown in Figure 4 and P_e is the probability of exceedance of $1 - F_x$ where $F_x$is the cumulative distribution function of x and α. x_0 is a constant for a given area (in this case $0.4m^2$ to $8m^2$). Typical distribution of peak ice pressures is shown in Figure 4 for different areas.

The constants α and x_0 can be determined from the fit-to-tail distribution of exceedance probability for each area as shown in Figure 5. However x_0 can be ignored if it is close to 0 or negative (Taylor et al., 2010). In this study, the influence of x_0 for all areas may be negligible because they are all negative values.

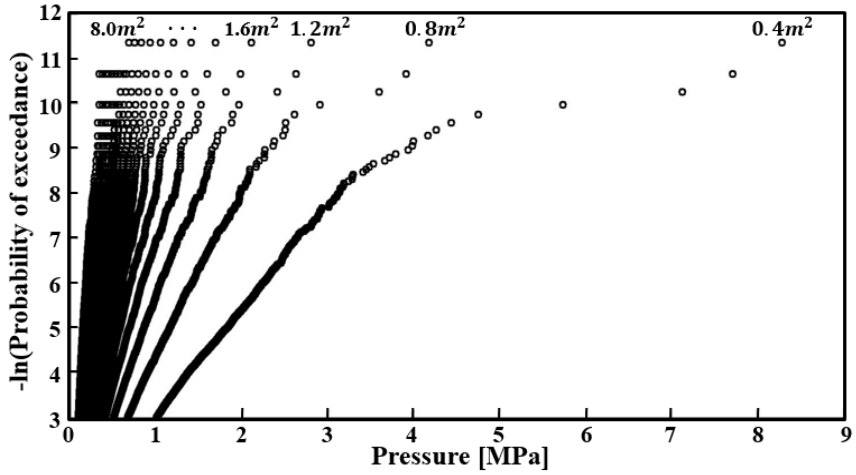

Figure 4. Ranked local pressure data measured onboard the ARAON for different areas $0.4m^2$ to $8m^2$

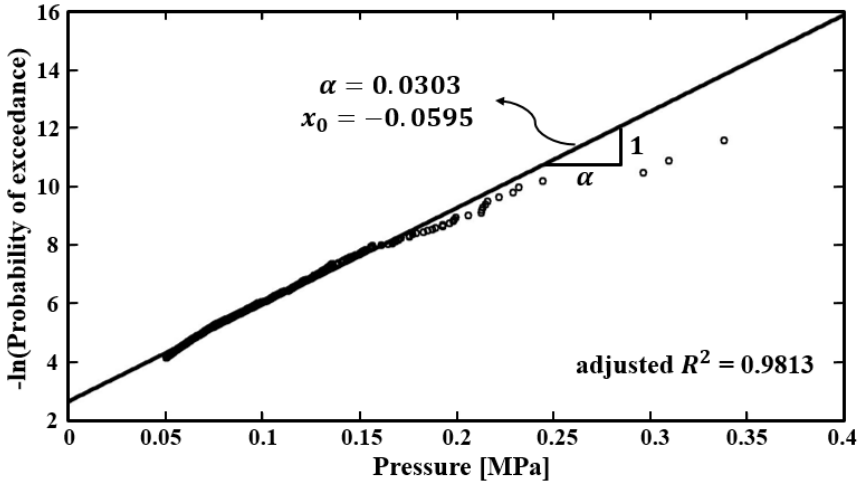

Figure 5. Determination of constants α and x_0 from fit to tail of peak ice pressure distribution for area $8m^2$

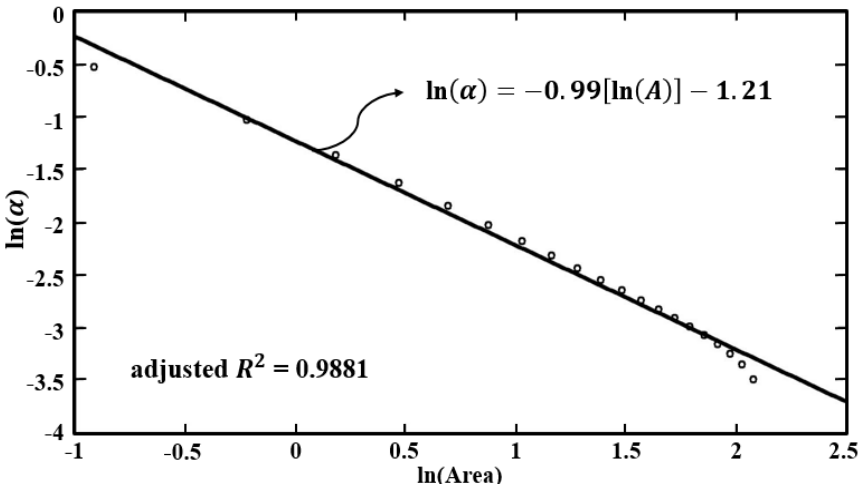

Figure 5. *ln*(Area) vs. *ln*(α)

All values α determined for each area are plotted in a log-log scale graph in Figure 6. A linear equation can be obtained from this distribution in log-log scale and eventually gives an exponential function as

$$\alpha = 0.29A^{-0.99} \tag{6}$$

In analyzing peak ice pressure data, the exposure of structure area and the number of events are important. The probability of peak ice pressure occurred per unit period can be expressed as a Poisson process, then the probability of exceedance function F_p as shown in Eq.(7).

$$F_p(p) = exp[-exp\left(-\frac{p - x_0}{\alpha}\right)\mu] \tag{7}$$

Here μ is the total number of events occurring over a unit period multiplied by the ratio of events occurring at the target area to the total event (Taylor et al., 2010).

Eq.(7) can be expressed for local ice pressures p as in Eq.(8) by substituting α

$$\mathrm{p} = 0.29A^{-0.99}[-ln(-ln\big(F_P(p)\big) + ln\,\mu] \text{ [MPa]} \tag{8}$$

The total measurement time of the ARAON's 2016 Arctic filed test was approximately 310hrs. There were 1,712 events and the average number of events was 5.5 per hour. Assuming the ARAON operates 1,000hrs a year, the average number of events during a year is 5,523. Therefore the peak ice pressure that can be occurred is shown in Figure 7. For design purpose the ice pressures corresponding to an excess of 1% do not cause fatal structural damage, hence it is reasonable to choose pressure level corresponding to 1% exceedance probability (Frederking, 2003). Eventually the local pressure prediction formula based on the field test of the ARAON can be represented as:

$$p_{0.01} = 3.93A^{-0.99} \text{ [MPa]} \tag{9}$$

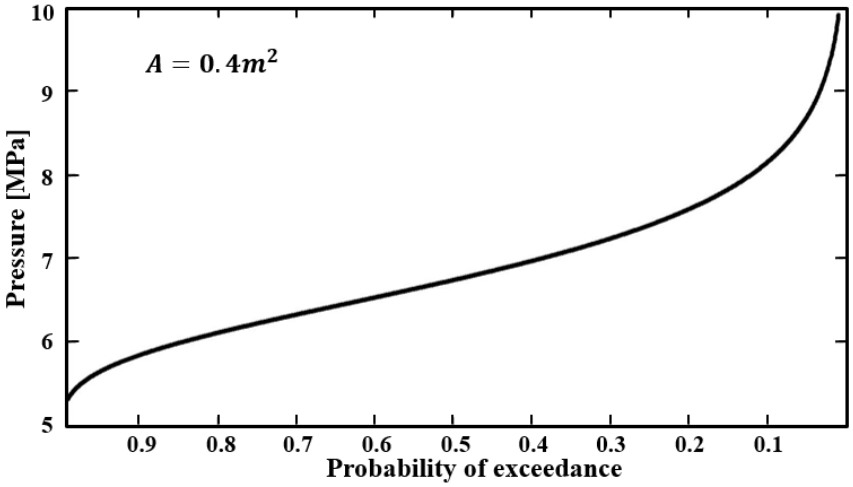

Figure 7. Probability of exceedance vs. peak ice pressure

4. Modification of pressure-area relationship

Eq.(9) is a very simple pressure-area relationship for the IBRV ARAON, where ice pressure is a function of contact area only. Eq.(9) may be used for the initial design stage of an icebreaker of similar size to the ARAON, however it may be more practical to include other ice-structure interaction factors in addition to contact area.

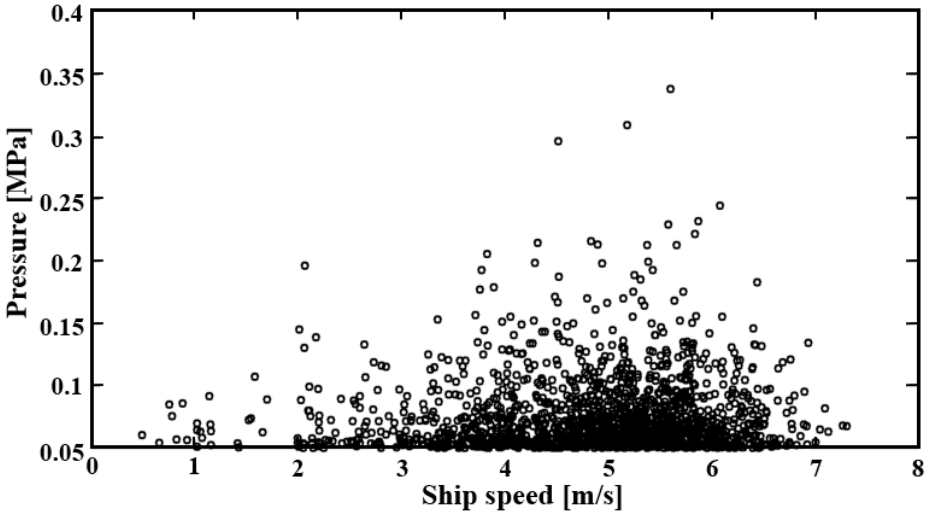

Figure 8. Ship speed against peak ice pressure for area $8m^2$

Figure 8 is a collection of data for the peak ice pressure against ship speed. Estimated peak pressure is dispersed over wide range of ship speed, but in general ice pressure increases as ship speed increases. In order to figure out ship speed effect on the peak ice pressure, Froude number was adopted to modify proposed local ice pressure equation.

$$Fr = \frac{V}{\sqrt{g \times L}} \tag{10}$$

where V is ship speed, g is gravitational acceleration, L is the characteristic length of ship, 110m for ARAON.

Figure 9 shows a log-log scale plot of the dimensionless pressure against Froude number. The outer limit straight line of data distribution can be chosen as a new expression for local ice pressure at given ship speed.

$$ln\left(\frac{Pressure}{p_{0.01}}\right) = 0.49\, ln(\frac{V}{\sqrt{gL}}) + 0.75 \tag{11}$$

Combining Eq.(11) with Eq.(9) gives a modified pressure-area relationship Eq.(12) for the ARAON which includes ship speed as a secondary design factor.

$$p'_{0.01} = 8.43A^{-0.99}(\frac{V}{\sqrt{gL}})^{0.49}\ \text{[MPa]} \tag{12}$$

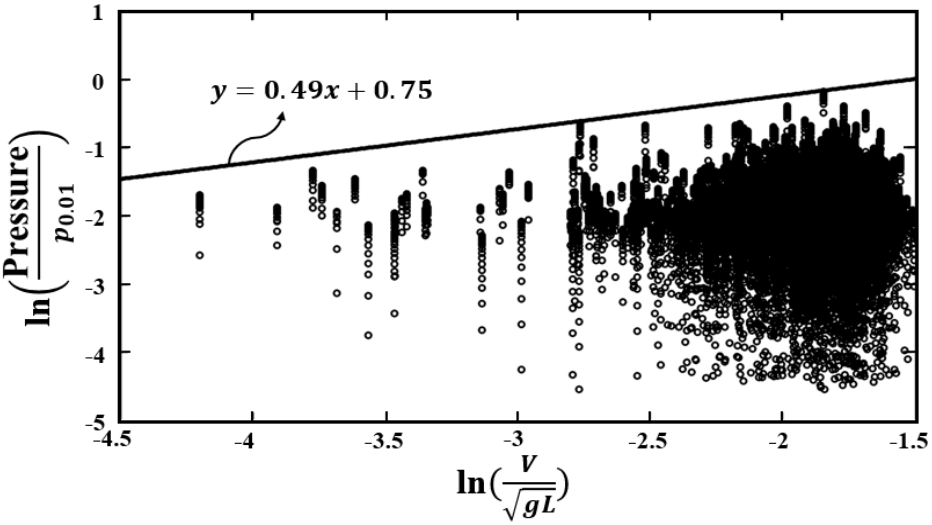

Figure 9. Relationship between peak ice pressure and ship speed

Ice pressure also tends to increase as ice thickness increases. Similarly the effect of ice thickness can be included and the dimensionless thickness parameter $\frac{h}{h_{ref}}$ was adopted to modify local ice pressure equation.

The outer limit straight line of local ice pressure data distribution shown in Figure 10 can be chosen as

$$ln\left(\frac{Pressure}{p'_{0.01}}\right) = 0.28\, ln(\frac{h}{h_{ref}}) - 1.01 \tag{13}$$

Combining Eq.(13) with Eq.(9) gives a modified pressure-area relationship Eq.(14) for the ARAON which includes ship speed and ice thickness.

$$p''_{0.01} = 6.96A^{-0.99}\left(\frac{V}{\sqrt{gL}}\right)^{0.49}\left(\frac{h}{h_{ref}}\right)^{0.28}\ [\text{MPa}] \tag{14}$$

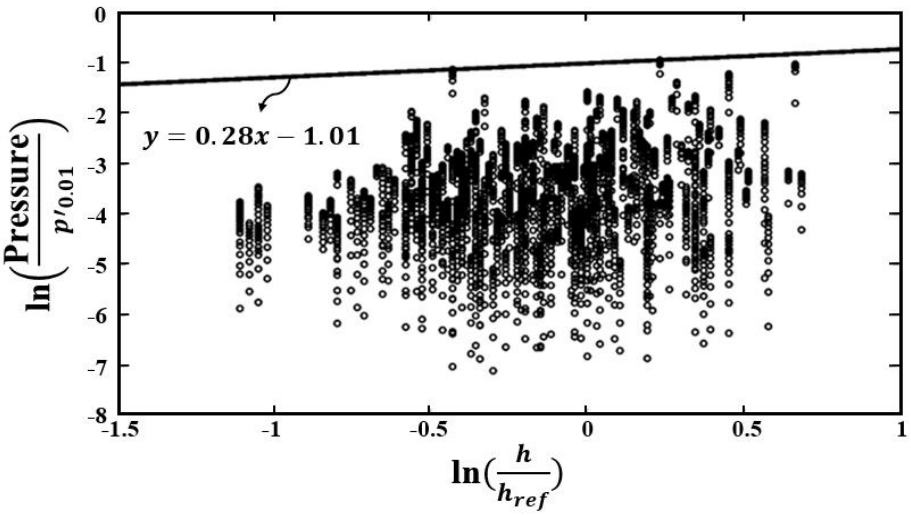

Figure 10. Relationship between peak ice pressure and ice thickness

Figure 11 show the result of modified pressure-area relationship Eq.(14) with the original ice pressure Eq.(9) in log-log scale. The modified equation reflects changes in ship speed. Similar results are derived for the ice thickness variation as shown in Figure 12.

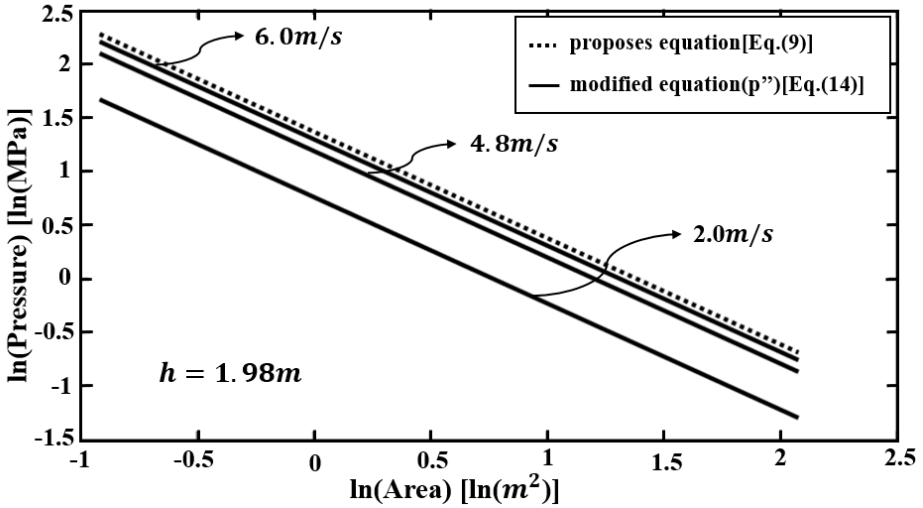

Figure 11. Modified ice pressure expression Eq.(14) with traditional relationship Eq.(9) with varying ship speed

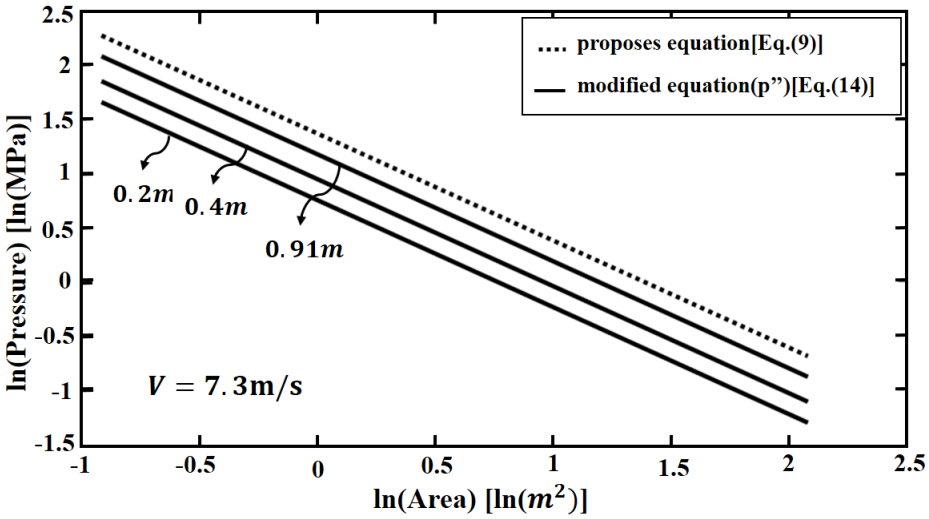

Figure 12. Modified ice pressure expression Eq.(14) with traditional relationship Eq.(9) with varying ice thickness

CONCLUSIONS

In this paper, the Arctic field test data from the IBRV ARAON's 2016 Arctic voyage were analyzed. A traditional pressure-area type relationship Eq.(9) is derived by applying probabilistic approaches to handle the measured strains and then is modified to consider other factors such as ship speed and ice thickness for local ice load prediction. Modified equation Eq.(14) can reflect changes in ship speed and ice thickness.

ACKNOWLEDGEMENTS

Research fund supported by Ministry of Trade, Industry and Energy of Korea (Project No.10063417) is greatly acknowledged.

REFERENCES

Frederking, R., 2003. Determination of Local Ice Pressures from Ship Transits in Ice. *Proceedings of 13th International Society of Offshore and Polar Engineering Conference*, Hawaii USA.

Frederking, R., 2004. Ice Pressure Variations during Indentation. *Proc. of IAHR Symposium on Ice*, pp.307-314.

Jeon, M.C., Min, J.K., Choi, K., & Ha, J.S., 2017. Estimation of Local Ice Load by Analyzing Shear Strain Data for the IBRV ARAON. *Proceedings of 24th Symposium on Port and Ocean Engineering under Arctic Conditions*, Busan Korea, 148.

Jordaan, I.J., Maes, M.A., Brown, P.W., & Hermans, I.P., 1993. Probabilistic Analysis of Local Ice Pressures. *Journal of Offshore Mechanics and Arctic Engineering*, 115(1), pp.83-89.

Lee, T.K., Kim, T.W., Rim, C.W., & Kim, S., 2013. A Study on Calculation of Local Ice

Pressures for ARAON Based on Data Measured at Arctic Sea. *Journal of Ocean Engineering and Technology*, 27(5), pp.88-92.

Masterson, D.M., & Frederking, R., 1993. Local Contact Pressures in Ship/Ice and Structure/Ice Interactions. *Cold Regions Science and Technology*, 21(2), pp.169-185.

Min, J.K., Choi, K., Cheon, E.J., & Kim, J.M., 2016. Ice Load Estimation Procedures for IBRV ARAON by Analyzing Shear Strain Data Measured in Arctic Sea. *Journal of Ocean Engineering and Technology*, 30(6), pp.468-473.

Park, I., Nam, J.H., Byun, S., & Park, J., 2014. Conversion of Pixel-based Ice Thickness to Physical Unit for Image of Broken Ice Patch. *Proceedings of the Society of CAD/CAM Conference*, pp.523-528.

Taylor, R.S., Jordaan, I.J., Li, C., & Sudom, D., 2010. Conversion of Pixel-based Ice Thickness to Physical Unit for Image of Broken Ice Patch. *Journal of Offshore Mechanics and Arctic Engineering*, 132(3)